Supporting Information

Abadir et al. 10.1073/pnas.1101507108

SI Methods

Isolation of Mitochondria. For functional assays, crude mitochondria from animal groups were separated by using differential centrifugation as described previously (1). Electron microscopy imaging and Western blot analysis of isolated mitochondria showed minimal contamination of the isolated mitochondria with other cell fractions.

For structural and morphological studies, mouse liver, heart, kidney, and brain cells were subjected to fractionation into whole-cell homogenate, postnuclear, crude mitochondria, density-purified mitochondria, mitoplast, and inner mitochondrial membrane fractions. Density-purified mitochondria were isolated on a discontinuous Percoll/HistoDenz gradient (2). Mitochondrial subfractions were prepared by sucrose density-gradient centrifugation essentially as described for pig heart mitochondria with minor variations (3). Briefly, gradient-pure mitochondria were subjected to hypotonic swelling in ~1.5 L of 20 mM KH_2PO_4 for 40 min, at which point they were centrifuged at 8,000 × *g* to pellet swollen mitoplasts. The swollen mitoplasts were resuspended in 250 mM sucrose homogenized with a dounce homogenizer to dislodge the outer mitochondrial membrane. The solution was layered onto a discontinuous sucrose gradient consisting of 25.2%, 37.7%, 51.7%, and 61.5% layers. Sucrose gradients were centrifuged at 77,000 × *g* for 90 min at 4 °C. Light membranes containing outer membrane markers were collected from the 37.7%/51.7% sucrose interface. This fraction is known hereafter as the outer mitochondrial membrane-enriched fraction. Mitoplasts were collected, diluted in 250 mM sucrose, and homogenized in a dounce homogenizer. The suspension was centrifuged at 100,000 × *g* for 30 min to pellet membranes. The supernatant (containing matrix proteins) was decanted. The pellet was resuspended in 10 mM Tris (pH 8.0)/250 mM sucrose, sonicated at 20 W for 1 min on ice, and then layered onto a second sucrose density gradient. The outer and inner mitochondrial membrane fractions were stored as frozen pellets at −80 °C until required.

Western Blot Analysis. Typically, 10 μg of protein from either tissue homogenates or mitochondrial preparations were isolated from mouse kidney, heart, or brain and resolved by 12% SDS/PAGE. Proteins were and transferred to nitrocellulose membranes by using the iBlot transfer apparatus (Invitrogen) for 7.5 min. Membranes were blocked with 5% skim milk in TBS at room temperature for 1 h. Each membrane was then incubated with one of the following primary antibodies at room temperature for 1 h to detect cell membrane, mitochondrial, outer mitochondrial membrane, and inner mitochondrial membrane markers, respectively: mouse monoclonal anti-Na^+/K^+ ATPase at a dilution of 1:500 in 2% skim milk/TBS with 0.1% (vol/vol) Tween-20 (TBS-T) (c4646; Santa Cruz Biotechnology); mouse monoclonal anti-cytochrome *c* oxidase (CoxIV) at a dilution of 1:500 in 2% skim milk/TBS-T (A-6403; Molecular Probes); mouse monoclonal anti–voltage-dependent anion channel (VDAC) at a dilution of 1:500 in 2% skim milk/TBS-T (A-31855; Invitrogen); and mouse monoclonal anti-ATP synthase β at a dilution of 1:2,500 in 2% skim milk/TBS-T (A-21350; Invitrogen). In addition, membranes were incubated with a rigorously validated, well-characterized anti-angiotensin (Ang) type 2 receptor (AT_2R) antibody (4–6) (sc-9040; Santa Cruz Biotechnology), anti-Ang (7–9) (Santa Cruz Biotechnology), and anti-Ang type 1 receptor (AT_1R) antibody (10) (Santa Cruz Biotechnology). To confirm the absence of cross-reactivity of these antibodies, we studied Chinese hamster ovary (CHO) cells lacking AT_1R and AT_2R. Using immunoblot detection, we were able to detect AT_1R and AT_2R in positive controls but not in the CHO cells. After washing with PBS, the membranes were further incubated with respective secondary antibodies conjugated with horseradish peroxidase (Dako) 1:1,000 in 2% skim milk/TBS-T at room temperature for 1 h. Immunoreactive protein bands were visualized on film (Kodak X-Omat AR5) with SuperSignal West Pico chemiluminescence substrate (Pierce Biotechnology).

Transfection of Human Fibroblast Cells. Human fibroblast cells maintained in antibiotic-free DMEM supplemented with 10% FBS (BioMedia) and 2 mM L-glutamine (Invitrogen) were seeded in 35-mm glass-bottom dishes. Human AT_2R cDNA was purchased from Invitrogen as a recombination ultimate human ORF. To construct a mammalian expression vector, the AT_2R cDNA was cloned into the destination vector, pcDNA-Dest53, to create a pcDNA-GFP AT_2R.

As a positive control, pcDNA-EGFP-C1 was used. As a negative control, pcDNA-Dest47 with a termination sequence was used. When AT_2R is expressed in the pcDNA-Dest47, the polymerase reads ATG2 sequence but, instead of making a fusion protein with Cycle 3 GFP, the ATG2 sequence is terminated, resulting in bicistronic construct expression of ATG2 and GFP.

Human fibroblast cells were transiently transfected with 1 μg of DNA of pcDNA-Cycle 3 GFP-AT_2R, positive control pcDNA-EGFP, or negative control pcDNA AT_2R-Cycle 3 GFP by using Lipofectamine transfection reagent. The expression of recombinant AT_2R with an N-terminal cycle 3 GFP was confirmed by RT-PCR and DNA sequencing. Images of transfected human fibroblast cells were acquired with the Zeiss Meta Confocal Laser Scanning Microscope System using AIM software. An Ar laser exciting at 488 nm and a red He/Ne laser at 543-nm wavelengths were used to obtain optical sections. Narrow-band emission filters (nm) were used to eliminate channel cross-talk, and a 1.0-μm confocal aperture was used to obtain *Z*-plane sections. Slides were imaged with a 100× oil-immersion plan apo objective lens (n.a., 1.4) through a Zeiss Axiovert inverted microscope.

Measurement of Nitric Oxide (NO) Production in Isolated Mitochondria. Kidney mitochondria were isolated by homogenization and differential centrifugation in a medium containing 3.4 mL of 1 M sucrose, 12 mL of 1 M mannitol, 2.5 mL of 1 M KCL, 1 M Tris·HCL, 0.5 mL of 1 M EDTA, 1.5 mL of 0.1 M EGTA, and 0.1% BSA (pH 7.4). Mitochondria were suspended in incubation solution. Total mitochondrial protein was determined by a Lowry Protein Assay Kit (Sigma-Aldrich).

To directly monitor real-time changes in NO production from isolated mitochondria in response to specific AT_2R agonists (CGP421140 at 10 nM and 100 nM) and antagonists (PD-123319 at 100 nM and 1 μM), the NO fluorescent molecular detection probe kit (Enzo Life Sciences) was used according to the manufacturer's instructions (11). Briefly, isolated mitochondria were incubated under normal tissue-culture conditions with non-fluorescent, cell-permeable NO detection dye that reacts with NO in the presence of O_2 with high specificity, sensitivity, and accuracy, yielding a water-insoluble red fluorescent product. Isolated mitochondria were then treated for 30 min with the NO scavenger 2-(4-carboxyphenyl)-4,4,5,5-tetramethylimidazoline-1-oxyl-3-oxide (c-PTIO) followed by a 15-min incubation with AT_2R agonists and/or antagonists. Separate positive control samples were treated with the NO inducer L-arginine, and neg-

ative control samples were generated by treatment with NO scavenger (c-PTIO). The fluorescent products were measured by using a reader equipped with Cyanine 5 (650/670 nm).

Immunolocalization of AT_1R, AT_2R, and Ang. Immunogold electron microscopy was performed as described (12). In brief, mouse tissues were fixed in 4% formaldehyde in 0.1 M sodium cacodylate supplemented with 3% sucrose (wt/vol) and 3 mM $CaCl_2$ and cryoprotected in 2.3 M sucrose overnight in polyvinylpyrrolidone (Sigma). Ultrathin sections were cut on a Leica Ultracut UCT microtome, and sections were placed on Formvar-coated nickel 200-mesh hexagonal grids. The sections were incubated in primary antibody against rabbit anti-AT_2R, goat anti-Ang, or goat anti-AT_1R antibody overnight at 4 °C at a concentration of 10 μg/mL. We used a rigorously validated, well-characterized anti-AT_2R antibody (4–6) (Santa Cruz Biotechnology), anti-Ang antibody (7–9) (Santa Cruz Biotechnology), and anti-AT_1R antibody (10) (Santa Cruz Biotechnology). To confirm the absence of cross-reactivity of these antibodies, we studied CHO cells lacking AT_2R. Using a Pierce immunoaffinity matrix with subsequent immunoblot detection, we were able to detect AT_2R in positive controls but not in the CHO cells.

Primary antibodies were detected with either 6-nm colloidal gold donkey anti-goat or 12-nm colloidal goat anti-rabbit (Jackson ImmunoResearch) diluted 1:20 in PBS for 1 h. Final contrasting of the sections was done by incubating them in 2% methyl cellulose (Sigma) and 0.3% uranyl acetate (Ted Pella) for 10 min at 4 °C. All sections were viewed with a Philips CM 120 TEM transmission electron microscope at an accelerating voltage of 80 kV. Images were taken with a Gatan Orius SC 1000 digital camera. Photographs for representative sections were taken.

Mitochondrial Respiration. For monitoring respiration, isolated mitochondria from rat heart or liver (10 μg of protein per well) were aliquoted into 96 wells of a polyethyleneimine-coated XF96 cell culture microplate (Seahorse Bioscience) (13). The plate was centrifuged at 3,000 × *g* for 10 min at 4 °C in an A-4-62 rotor, which control experiments determined caused an attachment of isolated mitochondria that was sufficiently robust to withstand the mixing protocols of the machine. Mitochondria were placed in 300 μL per well of mitochondrial buffer [20 mM Hepes, 137 mM KCl, 2.5 mM $MgCl_2$, 2 mM K_2HPO_4, 0.5 mM EGTA, and 0.2% (wt/vol) BSA (pH 7.3) at 37 °C]. Plates were used immediately. The cell culture microplate was incubated and loaded into the Seahorse XF96 extracellular flux analyzer following the manufacturer's instructions. All experiments were performed at 37 °C. Oxygen consumption rate data points refer to the mean rates during the measurement cycles, which consisted of a mixing time of 30 s and a wait time of 2 min followed by a data acquisition period of 10 min (50 data points). Mitochondrial substrates glutamate/malate (Sigma-Aldrich) or succinate (Sigma-Aldrich) were added to a final concentration of 5 mM. ADP (Sigma-Aldrich) was added to a final concentration of 1 mM. AT_2R agonist CGP421140 (Sigma-Aldrich) was added to a final concentration of 0.1 nM to 10 μM. AT_2R antagonist PD-123319 (Sigma-Aldrich) was added at a final concentration of 1 μM. An arginine analog that inhibits NO production, L-N^G-nitroarginine methyl ester (L-NAME; Sigma-Aldrich), was added at a final concentration of 1 μM. The oxygen consumption rates were determined by using a compartment model-based deconvolution algorithm, which compensated for oxygen diffusion phenomena occurring around the entrapped volume and for the response time of the probe.

Mitochondrial Membrane Potential and NADH Measurements. Inner membrane potential of isolated mitochondria ($\Delta\Psi_m$) was quantified ratiometrically in a wavelength-scanning fluorometer (QuantaMaster; Photon Technologies International) with tetramethylrhodamine methyl ester (TMRM) fluorescence, as described previously (14). Isolated mitochondria were equilibrated with 50 nmol/L TMRM in the incubation medium for 5 min. Changes in $\Delta\Psi_m$ with increasing concentrations of the AT_2R agonist CGP421140 were quantified from the TMRM fluorescence ratio (573/546 nm excitation ratio with 590 nm emission), with calibration constants previously determined for isolated mitochondria incubated under identical conditions. NADH fluorescence was measured simultaneously with 350-nm excitation and 450-nm emission wavelengths.

Human and Animal Groups. Mitochondria were studied in adult human monocytes (20–30 y old), adult human skeletal muscle tissue, adult rats (24 wk old), adult (20 wk old) and aged (70 wk old) mice, and a human cell line. Adult mice at 50 wk of age were treated with the AT_1R blocker losartan at doses of 40–60 mg/kg per day for 20 wk. All experiments were approved by the Johns Hopkins Animal Care and use Committee and the Johns Hopkins Institutional Review Board.

Weight, blood urea nitrogen, creatinine, and albumin were measured in adult (20 wk) and aged (70 wk) mice and in aged mice on losartan treatment. There was no significant difference in any of the above measured indices during the time of treatment (Fig. S3). As to additional characterization of animals used in this study, the dose of losartan used in this study led to a 10–15% decrease in blood pressure. We visually inspected each animal carcass after the dissection for any abnormalities. In our small sample (10 animals per group), we did not observe any evidence of malignancy. In addition, all of the animals in the control and treatment groups showed no evidence of decreased activity or illness.

Statistical Analyses. Each experiment was performed at least two times. Triplicate cultures were included in each treatment group. Data are expressed as means ± SD and analyzed with the one-way ANOVA program. Differences were considered significant at $P < 0.05$, as determined by the Student–Newman–Keuls method for pairwise multiple comparisons.

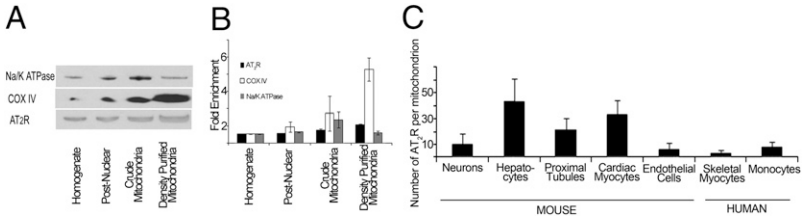

Fig. S1. *A* shows Western blot analysis of mouse heart whole cell homogenate fractionated up to a density purified mitochondria revealing that AT_2Rs track with mitochondrial marker Cox IV, consistent with mitochondrial enrichment. *B* shows integrated densitometric band analysis of immunoblots demonstrating fold enrichment of $mtAT_2Rs$, mitochondrial marker Cox IV, and cell membrane marker Na/K ATPase with mitochondrial purification. *C* is a bar graph representation of immune-labeling densities of $mtAT_2Rs$ in different mouse and human cell types. A total of 30 mitochondria from different sections of each immune labeling experiment were examined and the numbers of gold particles over each mitochondrion were then counted and averaged.

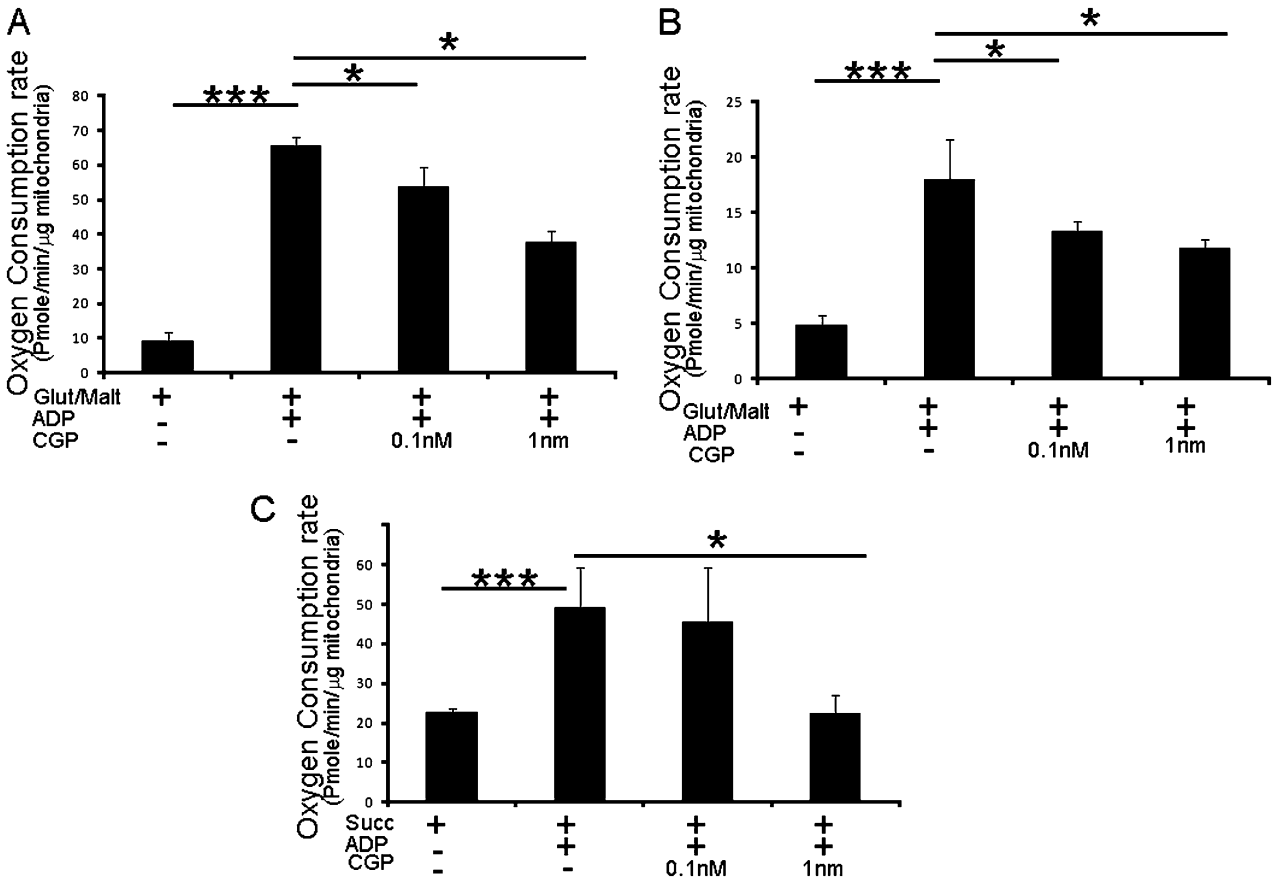

Fig. S2. Mitochondrial AT_2R activation inhibits mitochondrial respiration in mitochondria isolated from heart (*A*) and liver (*B* and *C*). (*A*) Respiration decreased significantly in response to AT_2R agonist CGP in cardiac mitochondria using glutamate/Malate as a substrate. (*B*) Respiration decreased significantly in response to AT2R agonist CGP in liver mitochondria using glutamate/Malate as a substrate. (*C*) Respiration decreased significantly in response to AT_2R agonist CGP in liver mitochondria using Succinate as a substrate. $*P < 0.05$, $**P < 0.005$, $***P < 0.0005$.

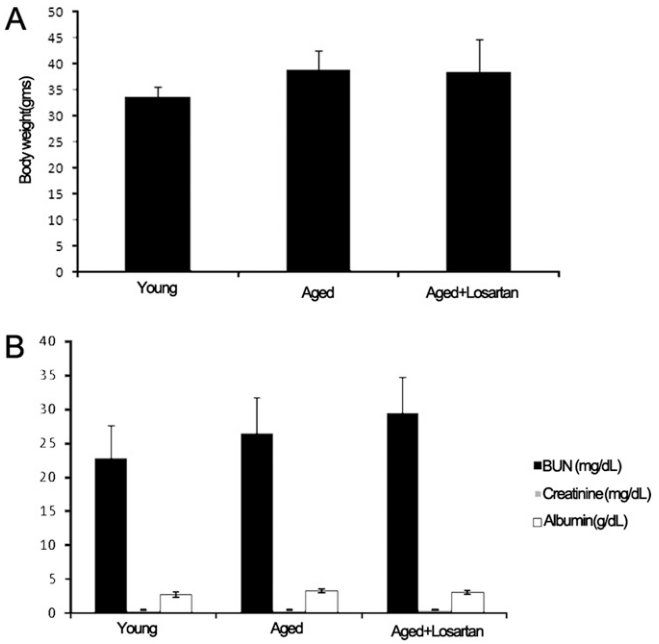

Fig. S3. (*A*) Mean weights in grams across treatment months between young, aged, and aged treated with losartan animals. (*B*) Mean blood urea nitrogen, creatinine, and albumin between young, aged, and aged treated with losartan animals (n = 10 in each group).

1. Cavadini P, Gakh O, Isaya G (2002) Protein import and processing reconstituted with isolated rat liver mitochondria and recombinant mitochondrial processing peptidase. *Methods* 26: 298–306.
2. Storrie B, Madden EA (1990) Isolation of subcellular organelles. *Methods Enzymol* 182:203–225.
3. Maisterrena B, Comte J, Gautheron DC (1974) Purification of pig heart mitochondrial membranes. Enzymatic and morphological characterization as compared to microsomes. *Biochim Biophys Acta* 367:115–126.
4. Lorenzo O, et al. (2002) Angiotensin III activates nuclear transcription factor-κB in cultured mesangial cells mainly via AT_2 receptors: Studies with AT_1 receptor-knockout mice. *J Am Soc Nephrol* 13:1162–1171.
5. Chan JY, Wang LL, Lee HY, Chan SH (2002) Augmented upregulation by c-*fos* of angiotensin subtype 1 receptor in nucleus tractus solitarii of spontaneously hypertensive rats. *Hypertension* 40:335–341.
6. Nagatsuka Y, et al. (2003) Carbohydrate-dependent signaling from the phosphatidylglucoside-based microdomain induces granulocytic differentiation of HL60 cells. *Proc Natl Acad Sci USA* 100:7454–7459.
7. Sakai K, et al. (2007) Local production of angiotensin II in the subfornical organ causes elevated drinking. *J Clin Invest* 117:1088–1095.
8. Thomas MA, Fleissner G, Stöhr M, Hauptfleisch S, Lemmer B (2004) Localization of components of the renin-angiotensin system in the suprachiasmatic nucleus of normotensive Sprague-Dawley rats: Part B. angiotensin II (AT_1)-receptors, a light and electron microscopic study. *Brain Res* 1008:224–235.
9. Thomas MA, Fleissner G, Stöhr M, Hauptfleisch S, Lemmer B (2004) Localization of components of the renin-angiotensin system in the suprachiasmatic nucleus of normotensive Sprague-Dawley rats: Part A. angiotensin I/II, a light and electron microscopic study. *Brain Res* 1008:212–223.
10. Ren L, et al. (2010) The inhibitory effects of rosiglitazone on cardiac hypertrophy through modulating the renin-angiotensin system in diet-induced hypercholesterolemic rats. *Cell Biochem Funct* 28:58–65.
11. Wardman P (2007) Fluorescent and luminescent probes for measurement of oxidative and nitrosative species in cells and tissues: Progress, pitfalls, and prospects. *Free Radic Biol Med* 43:995–1022.
12. Chen JQ, Delannoy M, Cooke C, Yager JD (2004) Mitochondrial localization of ERα and ERβ in human MCF7 cells. *Am J Physiol Endocrinol Metab* 286:E1011–E1022.
13. Choi SW, Gerencser AA, Nicholls DG (2009) Bioenergetic analysis of isolated cerebrocortical nerve terminals on a microgram scale: Spare respiratory capacity and stochastic mitochondrial failure. *J Neurochem* 109:1179–1191.
14. Scaduto RC., Jr., Grotyohann LW (1999) Measurement of mitochondrial membrane potential using fluorescent rhodamine derivatives. *Biophys J* 76:469–477.